Available online at www.sciencedirect.com
ScienceDirect
Journal of Sound and Vibration 306 (2007) 955–967
JOURNAL OF SOUND AND VIBRATION
www.elsevier.com/locate/jsvi

Short Communication

Dynamical behaviors of a fluid-conveying curved pipe subjected to motion constraints and harmonic excitation

Wang Lin*, Ni Qiao, Huang Yuying

Department of Mechanics, Huazhong University of Science and Technology, Wuhan 430074, People's Republic of China

Received 8 April 2007; received in revised form 20 June 2007; accepted 23 June 2007

Abstract

This paper investigates the nonlinear dynamics of a fluid-conveying curved pipe subjected to motion constraints and harmonic excitation. At first, the background theory for curved pipes conveying fluid with motion constraints is presented. Then, emphasis is placed on the possible nonlinear dynamic behaviors of a constrained curved pipe subject to a harmonic excitation. For such a forced dynamical system, calculations of bifurcation diagrams, phase-plane portraits, time responses, power spectrum diagrams and Poincare maps of the oscillations clearly establish the existence of the chaotic motions and quasi-periodic motions. Moreover, it is found that the route to chaos is through a sequence of period-doubling bifurcations. Finally, the difference in the nonlinear dynamics between the self-vibration system and forced system is further discussed.

1. Introduction

The vibration problem of a curved pipe conveying fluid has been investigated to a great extent in the past decades. Work on this topic appears to have started in the 1960s. The pioneering works on the stability of curved pipes conveying fluid concentrated on the linear problems [1]. The literature on the nonlinear vibrations of fluid conveying curved pipes is quite limited. Perhaps the earliest study on the nonlinear problem for the curved pipe was by Ko and Bert [2]. Subsequently, Ko and Bert [3] considered the first-order nonlinear interaction between the pipe structure and the flowing fluid and formulated the governing equations of motion for the in-plane vibrations of a circular-arc pipe containing flowing fluid. A notable work done by Dupuis and Rousselet [4] derived the nonlinear differential equations of motion of a fluid-conveying pipe by making use of the Newtonian approach. Recently, Ni et al. [5] investigated a fluid-conveying curved pipe with demisemi-arc shape. It should be noted that this curved pipe was placed on nonlinear foundations. Based on numerical analysis, three final steady states were detected, and chaotic transients found, as a function of the flow velocity parameter. More recently, Ni et al. [6] developed a fluid-conveying curved pipe model subject to motion constraints placed arbitrarily along the pipe axis. It was shown that chaotic motions may occur at sufficiently high flow velocities for such a self-vibration system.

*Corresponding author. Fax: +86 27 87543238.
E-mail address: wanglinfliping@sohu.com (W. Lin).

0022-460X/$ - see front matter © 2007 Elsevier Ltd. All rights reserved.
doi:10.1016/j.jsv.2007.06.046

The purpose of the present study is described as follows. First, the background theory for a fluid-conveying curved pipe with motion constraints will be given. This constrained pipe model corresponds to a self-vibration system. Second, the nonlinear behaviors for a self-vibration pipe system will be investigated, both for symmetric and asymmetric constraints. Third, the forced pipe system with motion constraints will be analyzed in detail. In the forced system, the curved pipe is subject to a harmonic excitation at the free end of the pipe. Fourth, the difference in the nonlinear dynamics between the self-vibration system and forced system will be further discussed.

2. Background theory

Consider a simple curved pipe system as shown in Fig. 1(a). This circular fluid-conveying curved pipe is subject to symmetric constraints placed arbitrarily along the pipe axis. It is noted that this pipe model has been developed in the study by Ni et al. [6]. In that paper, the curved pipe has a constant center-line radius R to a fixed geometric center of curvature at point O, as shown in Fig. 1(a). The motion constraints are placed at an angle θ_c as measured from the reference x-axis. Obviously, this pipe model corresponds to a self-vibration system. The analytical model consists of a curved pipe having a mass per unit length m_p, effective flexural rigidity EI, internal perimeter S, the internal cross-sectional area A and subtended angle θ_0. Moreover, the fluid is taken to be incompressible and in laminar flow with a mass per unit length m_f, and constant velocity V. The fluid pressure is denoted by p.

This may be a common pipe model, used as a typical structural element in engineering practice. However, the pipe will impact on the motion constraints when the pipe is vibrating. The effect of the motion constraints can be written as a cubic-spring restraining force (see Ref. [6]). For the in-plane vibrational motion of such a fluid–structure system, u and w correspond to the radial deflection and tangential displacement of the curved pipe, respectively. Hence, by assuming that there is no extension of the centerline of the curved pipe, the

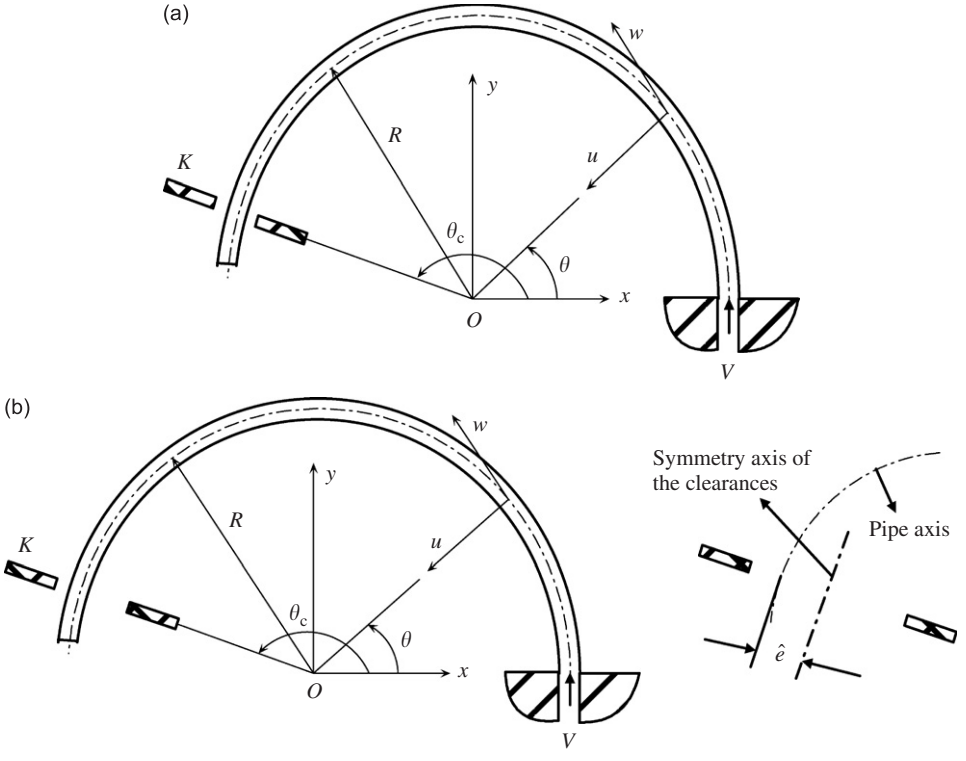

Fig. 1. Schematic of the self-vibration curved pipe system: (a) symmetric constraints and (b) asymmetric constraints.

equation of motion for such a curved pipe can be written in dimensionless form as follows [6]:

$$\frac{1}{\theta_0^6}\frac{\partial^6\xi}{\partial\varsigma^6}+(2+v^2)\frac{1}{\theta_0^4}\frac{\partial^4\xi}{\partial\varsigma^4}+(1+2v^2)\frac{1}{\theta_0^2}\frac{\partial^2\xi}{\partial\varsigma^2}+v^2\xi+2\beta^{1/2}v\frac{1}{\theta_0^3}\frac{\partial^4\xi}{\partial\tau\,\partial\varsigma^3}$$
$$+2\beta^{1/2}v\frac{1}{\theta_0}\frac{\partial^2\xi}{\partial\tau\,\partial\varsigma}+\frac{1}{\theta_0^2}\frac{\partial^4\xi}{\partial\tau^2\,\partial\varsigma^2}-\frac{\partial^2\xi}{\partial\tau^2}+3\left[k\frac{\partial^2\xi}{\partial\varsigma^2}\left(\frac{\partial\xi}{\partial\varsigma}\right)^2\right]\delta(\varsigma-\varsigma_c)+\left[k\left(\frac{\partial\xi}{\partial\varsigma}\right)^3\right]\frac{\partial\delta(\varsigma-\varsigma_c)}{\partial\varsigma}=0 \tag{1}$$

in which the dimensionless parameters are

$$\xi=w/R,\ \ \eta=u/R,\ \ \varsigma=\theta/\theta_0,\ \ \beta=m_f/(m_f+m_p),\ \ v=(m_f/EI)^{1/2}RV,$$
$$\tau=[EI/(m_f+m_p)]^{1/2}t/R^2,\ \ k=K(R^6/EI\theta_0^5),\ \ \varsigma_c=\theta_c/\theta_0.$$

In the above equation, K is the stiffness of the cubic spring which represents the effect of the motion constraints. It is noted that, compared with the linear equation of motion derived by Chen [7], the only nonlinearity in Eq. (1) is associated with the nonlinear constraints; hence, Eq. (1) should be valid only provided that the pipe motions are not too large. Another aspect is that this equation does not take into account the effect of steady-state axial tension and pressure that may cause a steady-state deformation of the curved pipe. Since the boundary conditions are clamped-free conditions, the steady-state axial tension-pressure force has a less pronounced effect on a clamped-free curved pipe [8,9]. Therefore, the use of Eq. (1) can reasonably capture the main characteristics of the cantilever system. One can also see the book by Paidoussis [1], which contains extensive discussion of various issues related to the modeling of fluid-conveying curved pipes.

Based on numerical calculations, Ni et al. [6] have detected the possible chaotic motions once the flow velocity is sufficiently above the threshold for flutter about the buckled state. Hence, the curved pipe model shown in Fig. 1(a) can display interesting dynamical behaviors.

Besides the case for the curved pipe with symmetric constraints (Fig. 1(a)), another curved pipe system with asymmetric constraints is also considered in this work, as shown in Fig. 1(b). The equation of motion for the curved pipe with asymmetric constraints can be derived by utilizing the same method (Newtonian method) given in Ref. [6]. This equation is

$$\frac{1}{\theta_0^6}\frac{\partial^6\xi}{\partial\varsigma^6}+(2+v^2)\frac{1}{\theta_0^4}\frac{\partial^4\xi}{\partial\varsigma^4}+(1+2v^2)\frac{1}{\theta_0^2}\frac{\partial^2\xi}{\partial\varsigma^2}+v^2\xi+2\beta^{1/2}v\frac{1}{\theta_0^3}\frac{\partial^4\xi}{\partial\tau\,\partial\varsigma^3}+2\beta^{1/2}v\frac{1}{\theta_0}\frac{\partial^2\xi}{\partial\tau\,\partial\varsigma}$$
$$+\frac{1}{\theta_0^2}\frac{\partial^4\xi}{\partial\tau^2\,\partial\varsigma^2}-\frac{\partial^2\xi}{\partial\tau^2}+3\left[k\frac{\partial^2\xi}{\partial\varsigma^2}\left(\frac{\partial\xi}{\partial\varsigma}-e\right)^2\right]\delta(\varsigma-\varsigma_c)+\left[k\left(\frac{\partial\xi}{\partial\varsigma}-e\right)^3\right]\frac{\partial\delta(\varsigma-\varsigma_c)}{\partial\varsigma}=0 \tag{2}$$

where $e=(\theta_0/R)\hat{e}$, and $\hat{e}$ denotes the offset of the asymmetric constraints (see Fig. 1(b)).

3. The forced curved pipe system

In this section, a semicircular fluid-conveying curved pipe is considered, as shown in Fig. 2. There exists a harmonic excitation at the free end of the pipe. We assume that the harmonic excitation has the following form:

$$F=D\cos(\Omega t). \tag{3}$$

For this forced system, the governing equation is the same as that represented by Eq. (2). The solution of this equation is associated with the boundary conditions of the pipe system. It is noted that the boundary conditions of the forced system are different from that of the self-vibration system. Let $\tilde{\psi}$, $\tilde{N}$, $\tilde{M}$, and $\tilde{Q}$ be the angle of rotation, axial force, bending moment and transverse shear force, respectively. For this forced pipe model, the boundary conditions to be satisfied are as follows:at the fixed end ($\theta=0$):

$$u=w=0,\quad \tilde{\psi}=\frac{\partial u}{R\,\partial\theta}=0, \tag{4}$$

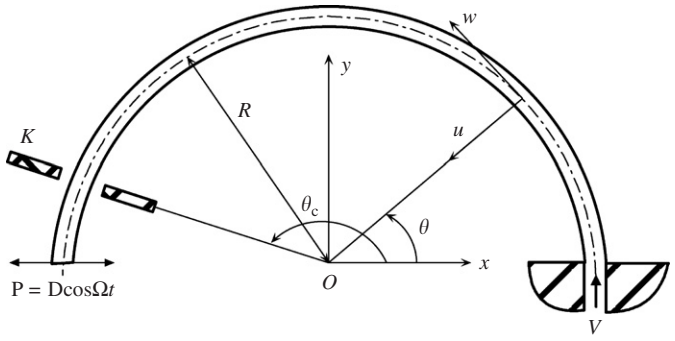

Fig. 2. Schematic of the forced-vibration curved pipe system.

at the free end ($\theta = \pi$):

$$\tilde{M} = \frac{EI}{R^2}\left(\frac{\partial^3 w}{\partial\theta^3} + \frac{\partial w}{\partial\theta}\right) = 0, \tag{5}$$

$$\tilde{Q} = \frac{EI}{R^3}\left(\frac{\partial^4 w}{\partial\theta^4} + \frac{\partial^2 w}{\partial\theta^2}\right) = D\cos(\Omega t), \tag{6}$$

$$\tilde{N}_\pi = \frac{EI}{R^4}\left(\frac{\partial^5 w}{\partial\theta^5} + 2\frac{\partial^3 w}{\partial\theta^3} + \frac{\partial w}{\partial\theta}\right) + \frac{m_f V^2}{R^2}\left(\frac{\partial^3 w}{\partial\theta^3} + \frac{\partial w}{\partial\theta}\right) + \frac{2m_f V}{R}\frac{\partial^3 w}{\partial\theta^2\,\partial t} + \frac{m_f V}{R}\frac{\partial w}{\partial t} + (m_f + m_p)\frac{\partial^3 w}{\partial\theta\,\partial t^2} + \frac{m_f V}{R}\left(\frac{\partial w}{\partial t} + V\right) = 0. \tag{7}$$

Note that the term on the right-hand side of Eq. (6), $D\cos(\Omega t)$, denotes the harmonic excitation at the free-end of the pipe. Thus the above boundary conditions can be rewritten as the dimensionless form:

$$\xi(0,\tau) = \eta(0,\tau) = \frac{\partial\eta(0,\tau)}{\partial\varsigma} = 0, \tag{8}$$

$$\frac{1}{\pi^3}\frac{\partial^3\xi(1,\tau)}{\partial\varsigma^3} + \frac{1}{\pi}\frac{\partial\xi(1,\tau)}{\partial\varsigma} = 0, \tag{9}$$

$$\frac{1}{\pi^4}\frac{\partial^4\xi(1,\tau)}{\partial\varsigma^4} + \frac{1}{\pi^2}\frac{\partial\xi^2(1,\tau)}{\partial\varsigma^2} = d\cos(\omega\tau), \tag{10}$$

$$\frac{1}{\pi^5}\frac{\partial^5\xi(1,\tau)}{\partial\varsigma^5} + \frac{1}{\pi^3}\frac{\partial\xi^3(1,\tau)}{\partial\varsigma^3} + 2\beta^{1/2}v\frac{1}{\pi^2}\frac{\partial\xi^3(1,\tau)}{\partial\tau\,\partial\varsigma^2} + 2\beta^{1/2}v\frac{\partial\xi(1,\tau)}{\partial\tau} + \frac{1}{\pi}\frac{\partial\xi^3(1,\tau)}{\partial\tau^2\,\partial\varsigma} + v^2 = 0, \tag{11}$$

where $d = DR^3/EI$ and $\omega = [(m_f + m_p)/EI]^{1/2}R^2\Omega$.

4. Discretization of the fluid-conveying curved pipe

In this section, the differential quadrature method (DQM) will be introduced to discretize the equations of the pipe model. The differential quadrature technique approximates the partial derivative of a function with respect to a space variable at a given discrete point as a weighted linear sum of the function values at all discrete points in the domain of that variable. This is in contrast to the finite difference method in which a solution value at a point is a function of values at adjacent points only. Even if the finite difference method is of high enough order to cover all points on the grid, a fundamental difference remains in that the method of differential quadrature is a polynomial fitting, while the higher-order finite difference method is a Taylor series expansion. Mathematically, the application of the differential quadrature method to a partial differential

equation can be expressed as follows:

$$L_k\{f(x)\}_i = \sum_{j=1}^{N} A_{ij}^{(k)} f(x_j), \tag{12}$$

where L denotes a differential operator, k is kth order of derivative, $x_j (j = 1,2, \ldots, N)$ are the discrete points considered in the domain, $f(x_j)$ are the function values at these points, $A_{ij}^{(k)}$ are the weighting coefficients attached to these function values, and N denotes the number of discrete points in the domain. Note that the weighting coefficients have been given by Bert and Malik [10].

For the curved pipe, the discrete points are in the domain of ς. By using the following method to discretize $\varsigma (0 \leqslant \varsigma \leqslant 1)$, one obtains the unequally spaced sampling points with three adjacent Δ-points ($\Delta = 10^{-6}$–10^{-3}) at the two boundary ends, namely

$$\begin{aligned} &\varsigma_1 = 0, \ \varsigma_2 = \Delta, \ \varsigma_3 = 2\Delta, \ \varsigma_{N-2} = 1 - 2\Delta, \ \varsigma_{N-1} = 1 - \Delta, \ \varsigma_N = 1, \\ &\varsigma_i = \frac{1}{2}\left[1 - \cos\left(\frac{i-3}{N-4}\pi\right)\right] \quad (i = 4, 5, \ldots, N-3). \end{aligned} \tag{13}$$

For simplicity, the motion constraints are applied at the point where $c = N-3$. Applying the DQM to Eqs. (1) and (2) yields

$$\begin{aligned} &\sum_{j=1}^{N}\left[\frac{1}{\pi^6}A_{ij}^{(6)} + \frac{1}{\pi^4}(2+v^2)A_{ij}^{(4)} + \frac{1}{\pi^2}(1+2v^2)A_{ij}^{(2)}\right]\xi_j + v^2\xi_i + 2\beta^{1/2}v\sum_{j=1}^{N}\left(\frac{1}{\pi^3}A_{ij}^{(3)} + \frac{1}{\pi}A_{ij}^{(1)}\right)\dot{\xi}_j \\ &\quad + \sum_{j=1}^{N}\frac{1}{\pi^2}A_{ij}^{(2)}\ddot{\xi}_j - \ddot{\xi}_i + 3k\left(\sum_{j=1}^{N}A_{cj}^{(1)}\xi_j\right)^2\left(\sum_{j=1}^{N}A_{cj}^{(2)}\xi_j\right) + kA_{cc}^{(1)}\left(\sum_{j=1}^{N}A_{cj}^{(1)}\xi_j\right)^2\left(\sum_{j=1}^{N}A_{cj}^{(1)}\xi_j\right) = 0 \\ &\quad (i = 4, 5, \ldots, N-3). \end{aligned} \tag{14a}$$

$$\begin{aligned} &\sum_{j=1}^{N}\left[\frac{1}{\pi^6}A_{ij}^{(6)} + \frac{1}{\pi^4}(2+v^2)A_{ij}^{(4)} + \frac{1}{\pi^2}(1+2v^2)A_{ij}^{(2)}\right]\xi_j + v^2\xi_i + 2\beta^{1/2}v\sum_{j=1}^{N}\left(\frac{1}{\pi^3}A_{ij}^{(3)} + \frac{1}{\pi}A_{ij}^{(1)}\right)\dot{\xi}_j \\ &\quad + \sum_{j=1}^{N}\frac{1}{\pi^2}A_{ij}^{(2)}\ddot{\xi}_j - \ddot{\xi}_i + 3k\left(\sum_{j=1}^{N}A_{cj}^{(1)}\xi_j - e\right)^2\left(\sum_{j=1}^{N}A_{cj}^{(2)}\xi_j\right) + kA_{cc}^{(1)}\left(\sum_{j=1}^{N}A_{cj}^{(1)}\xi_j - e\right)^2\left(\sum_{j=1}^{N}A_{cj}^{(1)}\xi_j - e\right) = 0 \\ &\quad (i = 4, 5, \ldots, N-3). \end{aligned} \tag{14b}$$

The boundary conditions of the forced pipe, given by Eqs. (8)–(11), can be expressed in the differential quadrature form as follows:

$$\xi_1 = 0, \ \sum_{j=1}^{N}A_{2j}^{(1)}\xi_j = 0, \ \sum_{j=1}^{N}A_{3j}^{(2)}\xi_j = 0, \tag{15}$$

$$\sum_{j=1}^{N}\frac{1}{\pi^3}A_{(N-2)j}^{(3)}\xi_j + \sum_{j=1}^{N}\frac{1}{\pi}A_{(N-2)j}^{(1)}\xi_j = 0, \tag{16}$$

$$\sum_{j=1}^{N}\frac{1}{\pi^4}A_{(N-1)j}^{(4)}\xi_j + \sum_{j=1}^{N}\frac{1}{\pi^2}A_{(N-1)j}^{(2)}\xi_j = d\cos(\omega\tau), \tag{17}$$

$$\sum_{j=1}^{N}\frac{1}{\pi^5}A_{Nj}^{(5)}\xi_j + \sum_{j=1}^{N}\frac{1}{\pi^3}A_{Nj}^{(3)}\xi_j + 2\beta^{1/2}v\sum_{j=1}^{N}\frac{1}{\pi^2}A_{Nj}^{(2)}\dot{\xi}_j + \dot{\xi}_N + \sum_{j=1}^{N}\frac{1}{\pi}A_{Nj}^{(1)}\ddot{\xi}_j + v^2 = 0. \tag{18}$$

Hence, by rearranging Eqs. (14b)–(18), an assembled form of the dynamic motion equation is given as follows:

$$[\mathbf{M}]\{\ddot{\xi}\} + [\mathbf{G}]\{\dot{\xi}\} + [\mathbf{K}]\{\xi\} = \{\mathbf{Q}\}, \tag{19}$$

in which $\{\xi\}$, $\{\dot{\xi}\}$, and $\{\ddot{\xi}\}$ are the structural displacement, velocity, and acceleration vectors, respectively; [**M**], [**G**], [**K**], and [**Q**] denote the structural mass matrix, damping matrix, stiffness matrix, and forcing vector, respectively. The matrix elements of [**G**] and [**K**] are the functions of dimensionless fluid speed v and mass ratio β. In addition, [**K**] can be written as

$$[\mathbf{K}] = [\mathbf{K}_l] + [\mathbf{K}_{nl}], \tag{20}$$

where $[\mathbf{K}_l]$ and $[\mathbf{K}_{nl}]$ are the linear and nonlinear terms of [**K**], respectively. Obviously, all the elements of [**M**], [**G**], [**K**], and [**Q**] can be obtained directly from Eqs. (14b)–(18). Eq. (19) is the nonlinear dynamic equation of motion for the curved pipe conveying fluid. By solving this equation one can determine the dynamic behavior of the curved pipe with specific values of system parameters.

It should be noted that, as mentioned previously, the tangential displacement and the radial displacement of the curved pipe are inter-related. If the time response of the tangential displacement is determined by solving Eq. (19), the radial displacement can be obtained by the following relationship:

$$\eta_i = \sum_{k=1}^{N} A_{ik}^{(1)} \xi_k \quad (i = 1, 2, \ldots, N). \tag{21}$$

5. Numerical analysis

In this section, it is of interest to investigate, in detail, what behaviors may occur when several parameter values are varied. For this purpose, the Newmark method and Newton–Raphson iterative technique were used to develop the procedure for such a fluid–structure interaction system governed by Eq. (19). Attention will be concentrated on the nonlinear dynamics of the constrained curved pipe, both without and with a harmonic excitation.

5.1. Without forcing function

In the nonlinear analysis, the nonlinear dynamics with no forcing function will be analyzed first, for the pipes with symmetric and asymmetric constraints. For this purpose, the bifurcation diagram is constructed based on numerical calculations. Construction of bifurcation diagrams is a standard approach used to analyze nonlinear systems. It provides a summary of essential dynamics and is therefore a useful tool for acquiring the overview.

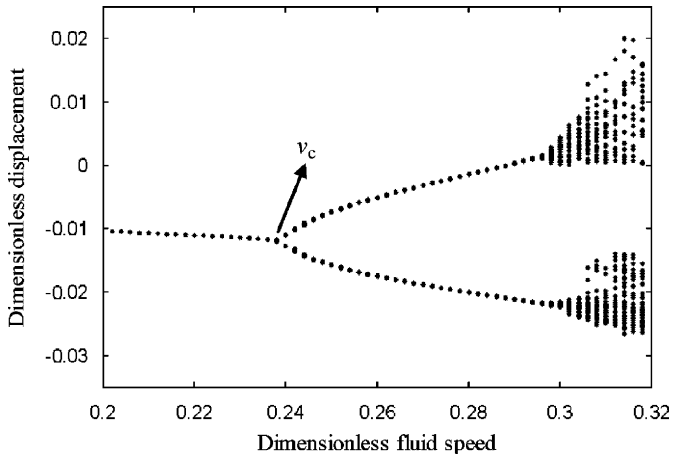

Fig. 3. Bifurcation diagram for the tip displacement of the nonlinear system defined by Eq. (22), as fluid speed is varied.

Calculations have produced the bifurcation diagram of Fig. 3 for a set of system parameters defined as follows:

$$\beta = 0.5,\ \ k = 1000,\ \ \varsigma_c = 0.854,\ \ N = 12,\ \ d = 0.0,\ \ \omega = 0,\ \ e = 0. \tag{22}$$

In the bifurcation diagram, the displacement plotted in the ordinate is the amplitude of the free-end displacement of the pipe. In the calculations, for clarity, the transient solutions were discarded. Then, whenever the free-end velocity, $\dot{\xi}(1,\tau)$, was zero, the displacement at the free end was recorded, as shown in Fig. 3. In this figure, the varied parameter is the dimensionless fluid speed v, and all the other parameters are defined by Eq. (22). From the bifurcation diagram, one can see that the solution of Eq. (19) corresponds to a steady-state solution when fluid speed is lower than $v_c = 0.2383$. It should be mentioned that, in the case of a low fluid speed, perhaps the system settles down onto one of the constraints with a negative static deflection (see Fig. 3). This phenomenon has also been observed experimentally in straight pipes conveying fluid [11]. However, when the fluid speed increases to $v_c = 0.2383$, an oscillatory motion can be detected. Furthermore, the amplitude of the oscillatory motion increases with increasing fluid speed. For a higher v, a sequence of period-doubling bifurcations can be detected. In Fig. 4(b–d), the period-1, -2, and chaotic motions are shown in the form of phase-plane portraits with various fluid velocities.

However, if the motion constraints are asymmetric ($e \neq 0$), it is found that the effect of the offset of the constraints on the dynamics of the pipe system is significant. Sample results are shown in Fig. 5. It is seen that the threshold v_c for the oscillatory motion is varied with various values of e.

For more details on the period-doubling bifurcations and chaos of this self-vibration system, one can refer to the foregoing study [6].

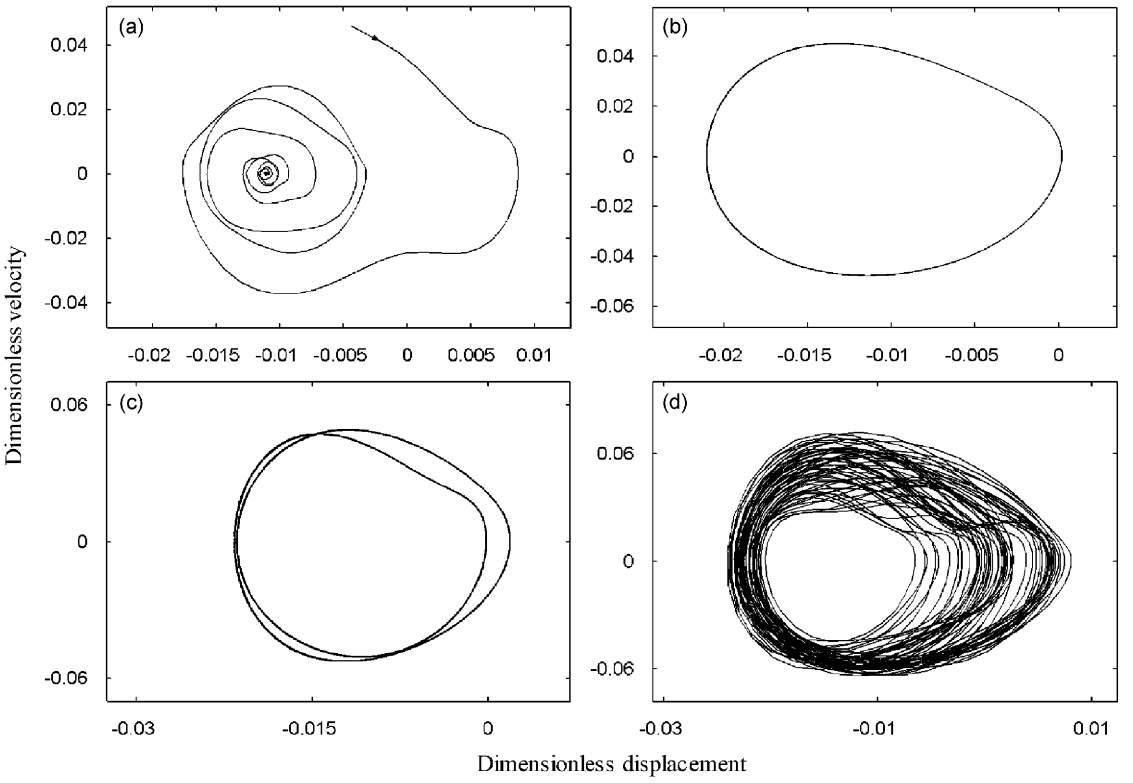

Fig. 4. Phase-plane plots of the free-end deflection of the pipe, for the system of Fig. 3, and various values of v: (a) $v = 0.22$, (b) $v = 0.29$, (c) $v = 0.295$, and (d) $v = 0.304$.

5.2. With forcing function

5.2.1. Bifurcation diagram

In the foregoing, the system with no forcing function was investigated, and the bifurcations and several motions were discussed. However, if the nonlinear system is subject to a harmonic excitation, this modified system may display much richer dynamics.

Similar bifurcation diagram (Fig. 6) may be constructed for a set of system parameters defined as follows:

$$\beta = 0.5,\ \ k = 1000,\ \ \varsigma_c = 0.854,\ \ N = 12,\ \ d = 0.005,\ \ \omega = 1,\ \ e = 0. \tag{23}$$

The remains of this section from this point, various dynamical behaviors shown in Fig. 6 will be discussed in detail. Obviously, in the results presented in Fig. 6, the harmonic excitation is a nonzero force. Except the forcing amplitude and frequency, all the other parameters utilized are the same as those defined by Eq. (22). From the bifurcation diagram, it is observed that, the varied parameter is the dimensionless fluid speed. It is seen that the curved pipe can display interesting dynamical behaviors, including chaotic, periodic, and quasi-periodic motions. However, the bifurcation diagram cannot distinguish chaotic responses from quasi-periodic ones.

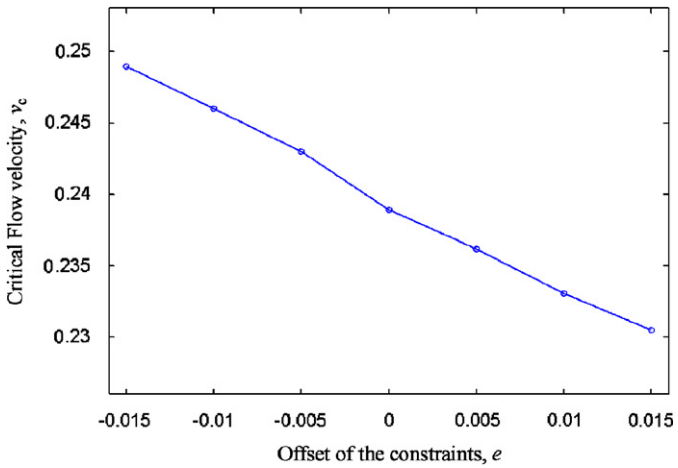

Fig. 5. The critical flow velocity with various values of e.

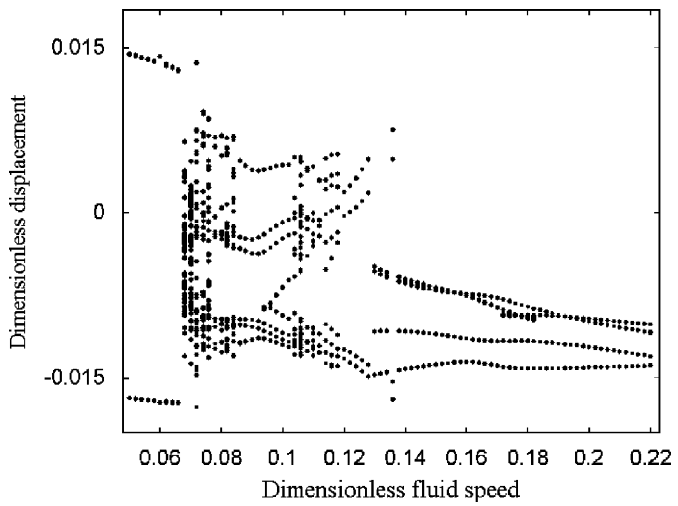

Fig. 6. Bifurcation diagram for the tip displacement of the nonlinear system defined by Eq. (23), as v is varied.

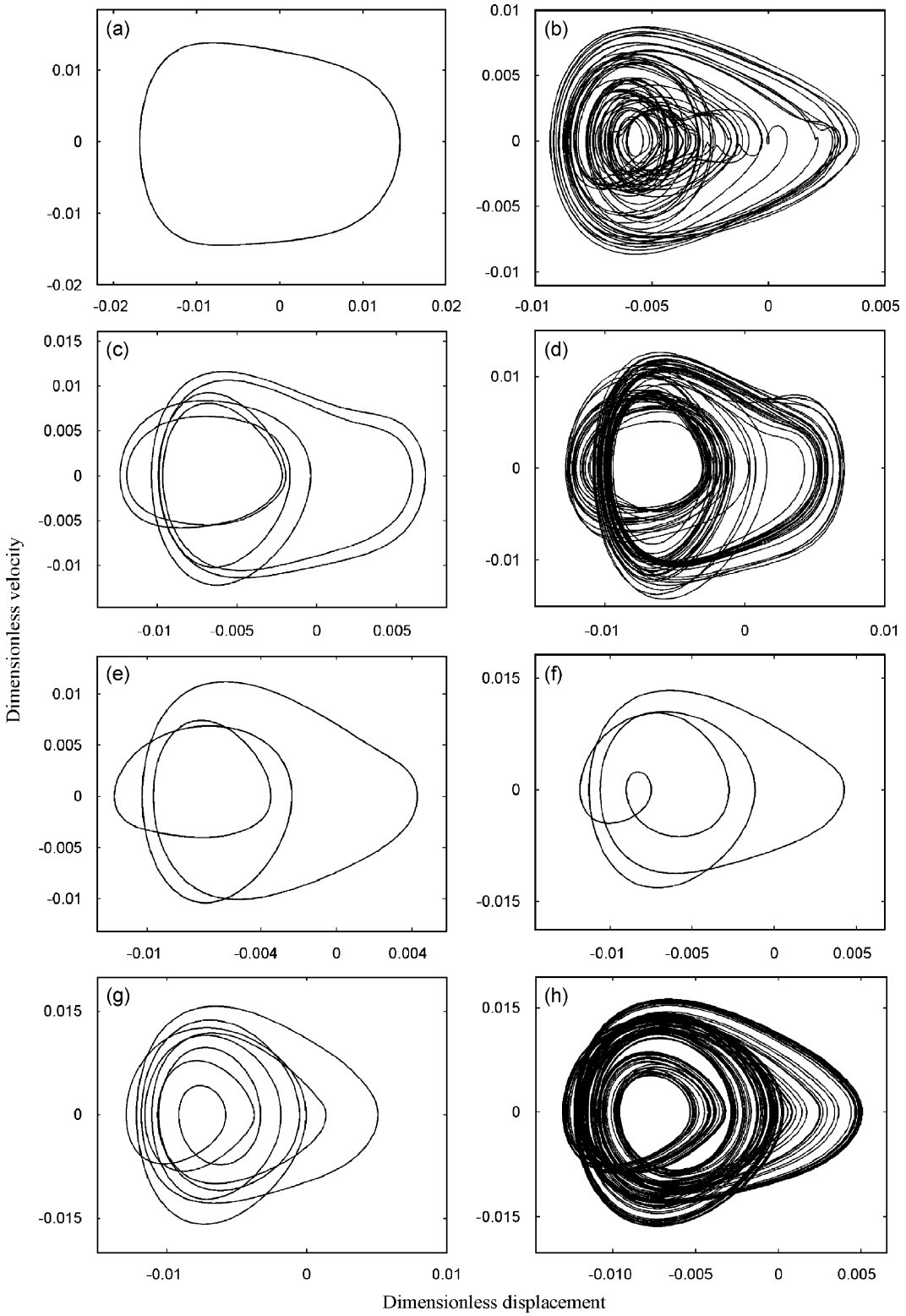

Fig. 7. Phase-plane plots of the free-end deflection of the pipe, for the system of Fig. 5, and various values of v: (a) $v = 0.05$, (b) $v = 0.068$, (c) $v = 0.078$, (d) $v = 0.082$, (e) $v = 0.088$, (f) $v = 0.098$, (g) $v = 0.104$, (h) $v = 0.106$, (i) $v = 0.130$, (j) $v = 0.220$, (k) $v = 0.240$, (l) $v = 0.260$, (m) $v = 0.270$, and (n) $v = 0.290$.

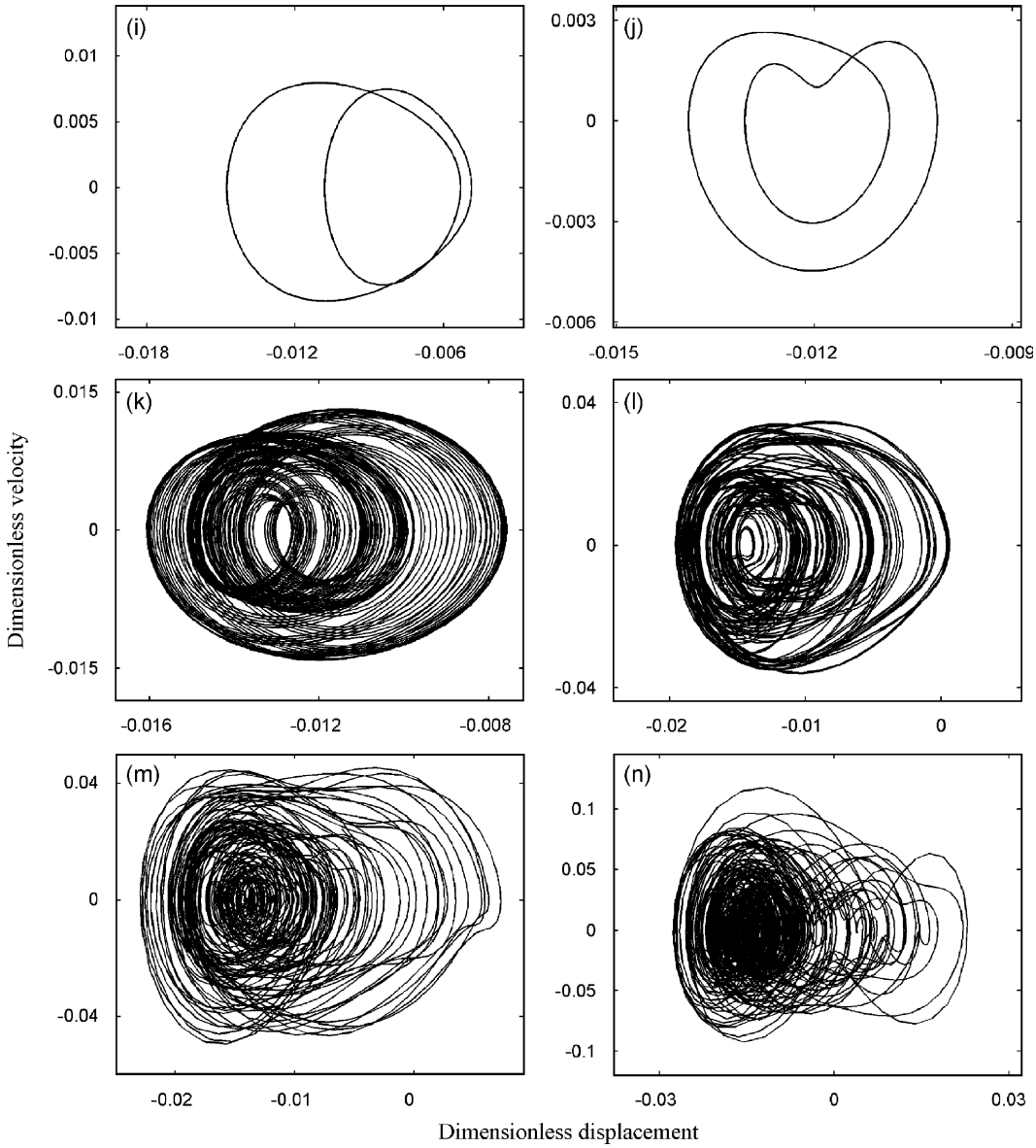

Fig. 7. (*Continued*)

5.2.2. Several dynamic motions

As mentioned in the foregoing, the vibration of the pipe undergoes complicated bifurcations as a function of v. In the following, it is instructive to look at several typical motions of the pipe system. For this purpose, the phase-plane portraits were constructed (see Fig. 7). It is seen in Fig. 7(a) that the trajectory is a stable oscillatory motion, which is asymmetric. The remaining parts of Fig. 7, show the following: (b), (d), (h), and (l)–(n) show chaotic motions with various values of v; (c), (e), (f), (g), (i), and (j) show, respectively, period-6, -3, -4, -8, -2, and -2 motions; (k) shows a quasi-periodic motion. The time responses, power spectrums and Poincare maps of several notable motions are shown in Figs. 8–10.

If the forcing frequency (ω) is chosen to be the variable parameter, and other parameters are fixed as defined in the foregoing and $v = 0.270$, quasi-periodic and chaotic motions can be found. Moreover, these two motions are detected to occur alternately as ω is varied continuously. Sample results are shown in Fig. 11.

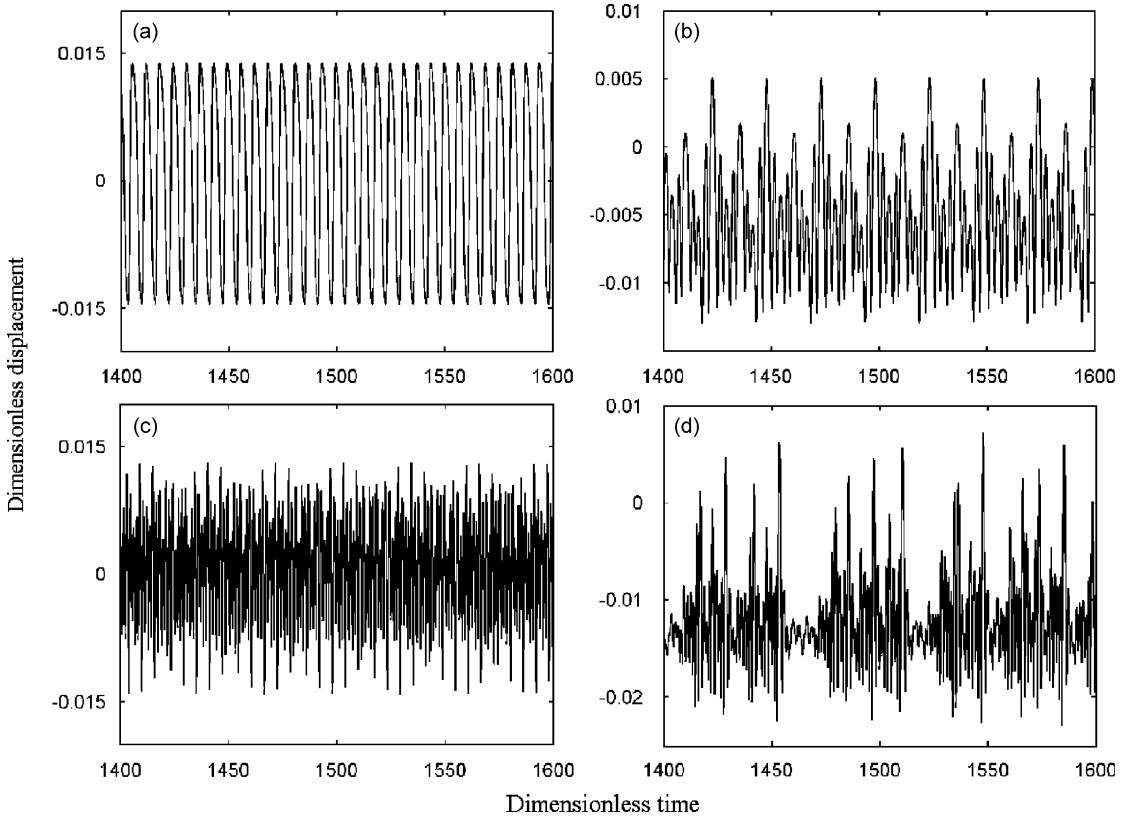

Fig. 8. Time responses for the free-end displacement of the pipe, for the system of Fig. 5. (a) $v = 0.05$, period-1 motion; (b) $v = 0.1046$, period-16 motion; (c) $v = 0.240$, quasi-periodic motion; (d) $v = 0.270$, chaotic motion.

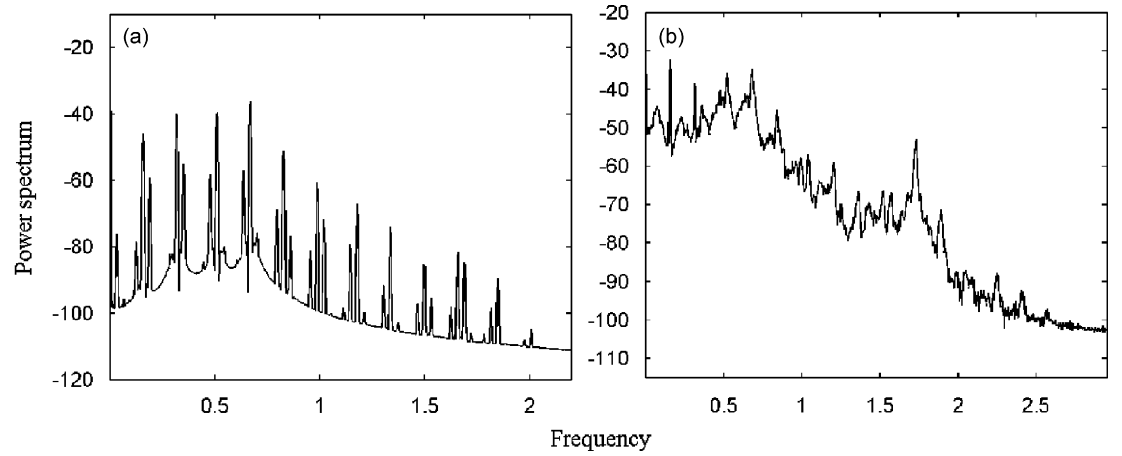

Fig. 9. Power spectrums of the vibration, for the system of Fig. 5: (a) $v = 0.240$ and (b) $v = 0.270$.

5.2.3. The route to chaos

In the numerical calculations, it is found that, as the parameter of v varies from a very small value to a reasonably large one, chaotic motions occur as the result of one route. From the bifurcation diagram, it can be seen that when the value of v varies in the range $0.09 < v < 0.1062$, a sequence of period-doubling bifurcations is detected, leading to a chaotic regime finally.

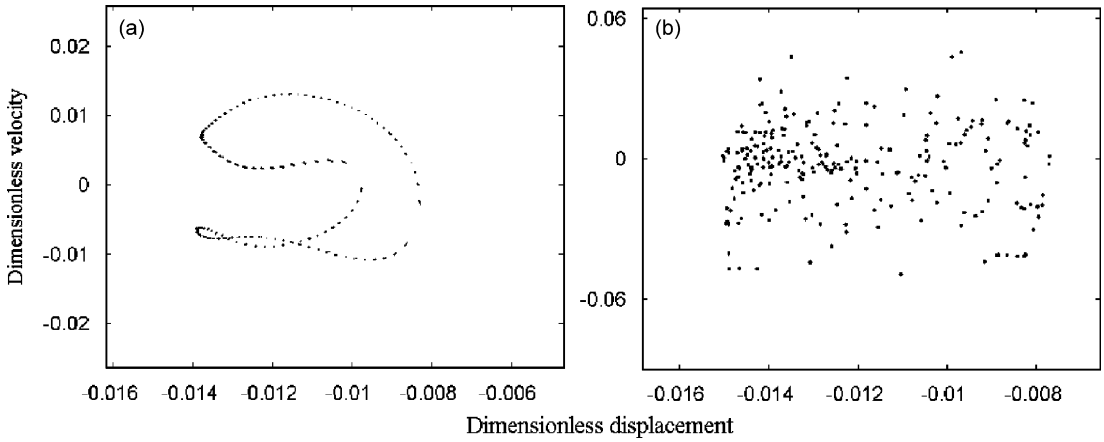

Fig. 10. Poincare maps for the free-end displacement and velocity, for the system of Fig. 5: (a) $v = 0.240$ and (b) $v = 0.270$.

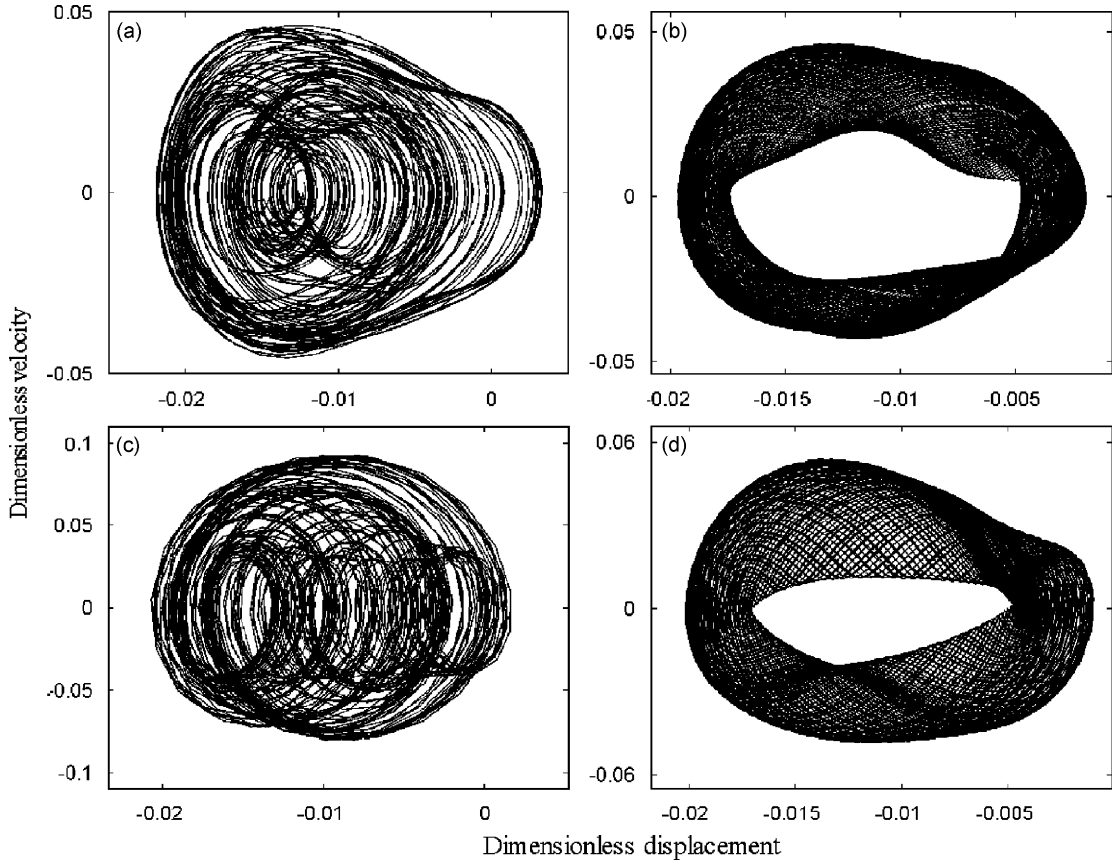

Fig. 11. Phase-plane plots of the free-end deflection of the pipe, for the system defined by $\beta = 0.5$, $k = 1000$, $\varsigma_c = 0.854$, $N = 12$, $d = 0.005$, $v = 0.27$, and various values of ω. (a) $\omega = 3.0$, chaotic motion; (b) $\omega = 10.0$, quasi-periodic motion; (c) $\omega = 11.0$, chaotic motion; (d) $\omega = 12.0$, quasi-periodic motion.

6. Discussion and conclusions

In this work, the nonlinear dynamics of a fluid-conveying curved pipe subjected to motion constraints (symmetric or asymmetric) and harmonic excitation has been investigated. Particular attention is concentrated on the possible existence of chaotic oscillations and several other interesting motions.

The equation of motion is discretized by differential quadrature method and then the nonlinear second-order ordinary differential equation system of Eq. (19) is numerically solved by Newmark method and Newton–Raphson iterative technique. Two variants of the basic system were considered, respectively. One is a curved pipe system with motion constraints and a harmonic excitation, another one is a curved pipe system with motion constraints but without harmonic excitation. Construction of bifurcation diagrams with the fluid speed v as parameter has shown that chaotic motions do indeed occur in the nonlinear system, both for the systems with and without harmonic excitation. The route to chaos is shown to be following a sequence of period-doubling bifurcations. However, for the forced pipe system, quasi-periodic motions may occur. Particularly, the curved pipe with harmonic excitation may undergo chaotic motions even if the flow velocity is very low (e.g., $v = 0.082$). Therefore, there exist strong contrasts between these two variants of the curved pipe system.

Thus, the analytical curved pipe model developed here is remarkably simple, and the numerical simulations are easy to implement. However, this system offers the potential for further and more profound theoretical and experimental studies into unexplored aspects of its dynamical behavior—which are currently being investigated.

Acknowledgments

The research was partially supported by the National Natural Science Foundation of China (No. 10272051) and the Science Foundation of HUST (No. 2006Q003B). The comments and suggestions made by the anonymous referees are also gratefully appreciated.

References

[1] M.P. Paidoussis, *Fluid–Structure Interactions: Slender Structures and Axial Flow*, Vol. 1, Academic Press, London, 1998.
[2] C.L. Ko, C.W. Bert, Non-linear vibration of uniformly curved, fluid-conveying pipes, *Proceedings of the Fifth International Conference on Pressure Vessel Technology*, San Francisco, CA, 1984, pp. 469–477.
[3] C.L. Ko, C.W. Bert, A perturbation solution for non-linear vibration of uniformly curved pipes conveying fluid, *International Journal of Non-linear Mechanics* 21 (1986) 315–325.
[4] C. Dupuis, J. Rousselet, The equations of motion of curved pipes conveying fluid, *Journal of Sound and Vibration* 153 (1992) 473–489.
[5] Q. Ni, L. Wang, Q. Qian, Chaotic transients in a curved fluid conveying tube, *Acta Mechanica Solida Sinica* 18 (3) (2005) 207–214.
[6] Q. Ni, L. Wang, Q. Qian, Bifurcations and chaotic motions of a curved pipe conveying fluid with nonlinear constraints, *Computers and Structures* 84 (2006) 708–717.
[7] S.S. Chen, Vibration and stability of a uniformly curved tube conveying fluid, *Journal of Acoustical Society of America* 51 (1972) 223–232.
[8] A.K. Misra, M.P. Paidoussis, K.S. Van, On the dynamics of curved pipes transporting fluid, part I: inextensible theory, *Journal of Fluids and Structures* 2 (1988) 221–244.
[9] A.K. Misra, M.P. Paidoussis, K.S. Van, On the dynamics of curved pipes transporting fluid, part II: extensible theory, *Journal of Fluids and Structures* 2 (1988) 245–261.
[10] C.W. Bert, M. Malik, Differential quadrature method in computational mechanics: a review, *Applied Mechanics Review* 49 (1996) 1–27.
[11] M.P. Paidoussis, C. Semler, Nonlinear and chaotic oscillations of a constrained cantilevered pipe conveying fluid: a full nonlinear analysis, *Nonlinear Dynamics* 4 (1993) 655–670.